Journal of Oceanography, Vol. 62, pp. 413 to 426, 2006

Seasonal Variations of the Ocean Surface Circulation in the Vicinity of Palau

Scott F. Heron[1]*, E. Joseph Metzger[2] and William J. Skirving[1]

[1]*Coral Reef Watch, NOAA/NESDIS/ORA, E/RA31, SSMC1, 1335 East-West Highway, Silver Spring, MD 20910, U.S.A.*
[2]*Naval Research Laboratory, Stennis Space Center, MS 39529-5004, U.S.A.*

(Received 2 August 2005; in revised form 17 January 2006; accepted 18 January 2006)

The surface circulation in the western equatorial Pacific Ocean is investigated with the aim of describing intra-annual variations near Palau (134°30′ E, 7°30′ N). *In situ* data and model output from the Ocean Surface Currents Analysis—Real-time, TRIangle Trans-Ocean buoy Network, Naval Research Laboratory Layered Ocean Model and the Joint Archive for Shipboard ADCP are examined and compared. Known major currents and eddies of the western equatorial Pacific are observed and discussed, and previously undocumented features are identified and named (Palau Eddy, Caroline Eddy, Micronesian Eddy). The circulation at Palau follows a seasonal variation aligned with that of the Asian monsoon (December–April; July–October) and is driven by the major circulation features. From December to April, currents around Palau are generally directed northward with speeds of approximately 20 cm/s, influenced by the North Equatorial Counter-Current and the Mindanao Eddy. The current direction turns slightly clockwise through this boreal winter period, due to the northern migration of the Mindanao Eddy. During April–May, the current west of Palau is reduced to 15 cm/s as the Mindanao Eddy weakens. East of Palau, a cyclonic eddy (Palau Eddy) forms producing southward flow of around 25 cm/s. The flow during the period July to September is disordered with no influence from major circulation features. The current is generally northward west of Palau and southward to the east, each with speeds on the order of 5 cm/s. During October, as the Palau Eddy reforms, the southward current to the east of Palau increases to 15 cm/s. During November, the circulation transitions to the north-directed winter regime.

Keywords:
· Ocean surface circulation,
· seasonal variation,
· western equatorial Pacific,
· Palau.

1. Introduction

The western equatorial Pacific Ocean is a key region of the world for climate studies that is difficult to describe due to its highly variable nature. Descriptions of the general circulation in the western equatorial Pacific Ocean that have focused on the major current systems of the North Equatorial Current (NEC), the Mindanao Current (MC), the Kuroshio, the North Equatorial Counter-Current (NECC) and the Indonesian Through-Flow (ITF) include the work of Toole *et al.* (1988), Lukas (1988), Lukas *et al.* (1991), Qu *et al.* (1998) and Qu and Lukas (2003). Two major mesoscale eddies reported in this region are the Mindanao Eddy (ME) and Halmahera Eddy (HE). Specific studies have examined the high- and low-frequency variability of these features (e.g., Lukas, 1988; Arief and Murray, 1996; Qiu and Lukas, 1996; Kashino *et al.*, 2001; Yaremchuk and Qu, 2004). Circulation studies in basins adjacent to the western Pacific have also been undertaken, e.g., the South China Sea (Metzger, 2003), and the Celebes and Maluku Seas (Kashino *et al.*, 2001). Lukas *et al.* (1991) described observations of current measurements from the Western Equatorial Pacific Ocean Circulation Study (WEPOCS) III conducted in the middle of 1988. Surface drifter and acoustic Doppler current profiler (ADCP) data were combined to produce a map of ocean currents that clearly showed the MC, ME, HE, NECC and portions of the ITF. Metzger *et al.* (1992) used these data as validation in a global ocean model. The model generated the same features from the WEPOCS III data with good effect and supplied further circulation detail in data-barren regions.

* Corresponding author. E-mail: Scott.Heron@noaa.gov

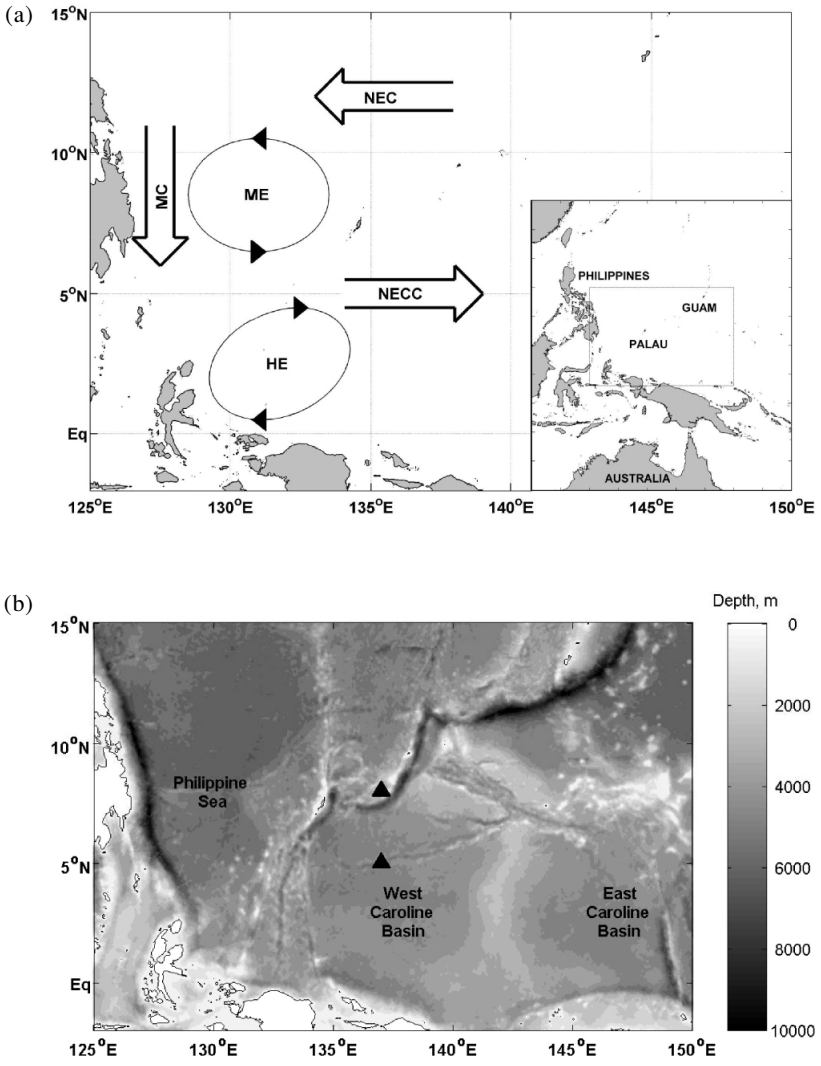

Fig. 1. (a) Schematic of the major ocean circulation features within the study area. Inset shows the geography of the western equatorial Pacific Ocean, with the study area indicated by the dashed box. (b) Smith and Sandwell (1997) bathymetry of study area. Triangles indicate the locations of TRITON buoys from which data are used.

However, to our knowledge, no existing investigations have focused on the circulation patterns in the immediate vicinity around Palau. The western equatorial Pacific is of significant interest in global ocean dynamics and the transport of waters in this region is important in understanding mass, heat and salt exchange. Physical connectivity of the remote Micronesian islands is an important factor for biological development; coral distribution and fish migration and reproduction are examples of biological processes that depend on physical ocean parameters.

The major islands of Palau are grouped together in the western Pacific Ocean 850 km east of the Philippine island of Mindanao, near 7°30′ N, 134°30′ E. Figure 1(a) shows the location of Palau and schematically illustrates the reported oceanographic features previously mentioned. These islands are at the peak of a topographic ridge that stretches to the SSW where the smaller island groups of Palau are found. This ridge separates the waters surrounding Palau into the Philippine Sea to the west of Palau, and the West Caroline Basin. Figure 1(b) shows the bathymetry of the western equatorial Pacific from the two-minute resolution data of Smith and Sandwell (1997). A rapid drop-off from the Palau Ridge to depths greater than 4000 m can be seen immediately to the east and west.

This work investigates seasonal characteristics of the ocean surface circulation in the region surrounding Palau. Existing satellite-derived and *in situ* data are collated and examined to identify general circulation features. Due to the spatially and temporally sparse nature of oceanographic data, particularly in the western equatorial Pa-

cific, output from a numerical model is also studied. To describe the ocean circulation near Palau, it is pertinent to first examine the larger scale features that may influence the Palauan waters. Thus, this study includes the ocean region bounded by 125–150°E and 2°S–15°N, as illustrated in Fig. 1(a).

The sources from which data were acquired to study the surface circulation are described in Section 2. The observations from each data source are summarized in Section 3 and then compared in Section 4 to determine consistency in the flow description. Section 5 summarizes the seasonal variations observed in surface waters around Palau.

2. Data Sources

2.1 Ocean Surface Currents Analyses—Real-time (OSCAR)

The Ocean Surface Currents Analyses—Real-time (OSCAR) derives sea surface currents from satellite observations for the global ocean, as described in Bonjean and Lagerloef (2002). Altimeter-derived sea surface height (SSH) and winds from scatterometer data are the primary input sources to OSCAR, with sea surface temperature (SST) data used as a secondary source. The SSH is gridded to 1° resolution, smoothed and then used to calculate geostrophic motion. This is linearly combined with the wind-driven (Stommel/Ekman) component. The accuracy of the OSCAR system is still under investigation. Surface current data were downloaded from the OSCAR website, http://www.oscar.noaa.gov. The time resolution is defined by the repeat period of the satellites, the minimum of which is 10-days for Jason-1. The database spanned eleven complete years, 1993–2003.

2.2 TRIangle Trans-Ocean buoy Network (TRITON)

The TRIangle Trans-Ocean buoy Network (TRITON) is a series of eighteen buoys deployed in the equatorial regions of the Pacific and Indian Oceans (http://www.jamstec.go.jp/jamstec/TRITON/). Mounted instruments provide information on the upper-ocean and surface meteorology. Surface wind data recorded by two TRITON buoys, located in the vicinity of Palau, were accessed from the TRITON website. The TRITON buoys located at 8°N, 137°E and 5°N, 137°E (Fig. 1(b)) provide the only *in situ*, extended observational data record near to Palau. However, the datasets from these buoys only span the periods of September 2001 to June 2003 and September 2001 to November 2003, respectively. The wind speed and direction were measured at a height of 4 m from the ocean surface and were sampled once every 5 seconds for a period of two minutes. The two-minute averages were recorded every ten minutes. Six such records were then averaged and published on the website as hourly means. To examine seasonal variability in the wind field, the hourly mean data were smoothed to eliminate high-frequency components.

2.3 NRL Layered Ocean Model (NLOM)

Output from the Naval Research Laboratory (NRL) Layered Ocean Model (NLOM) is also examined for the study region. NLOM is part of a real-time, eddy-resolving, nearly global ocean nowcast/forecast system (http://www7320.nrlssc.navy.mil/global_nlom) running daily at the Naval Oceanographic Office. It has a horizontal resolution of 1/16° and seven layers in the vertical, including a Kraus-Turner type bulk mixed layer. The model is forced with winds and heat fluxes from the Fleet Numerical Meteorology and Oceanography Center (FNMOC) Navy Operational Global Atmospheric Prediction System. It assimilates SST from satellite infrared data and SSH from satellite altimeter (TOPEX/POSEIDON, ERS-2 and Geosat Follow-On) data. Velocity fields are updated using a geostrophic correction calculated from pressure changes, but not within 5° of the equator. Between 5–8°, the correction is gradually increased to full strength using a hyperbolic tangent function. The entire system has been described in detail by Smedstad *et al*. (2003). The output used here is not from the operational model itself, but from a simulation system nearly identical to it. A hindcast reanalysis experiment was performed over the period 1993–2000 making use of all available satellite altimeter data.

2.4 Joint Archive for Shipboard ADCP Data (JASADCP)

ADCP data were downloaded from the Joint Archive for Shipboard ADCP website (http://ilikai.soest.hawaii.edu/sadcp) and collated for use as validation against the NLOM output. Thirty-one cruises passed through the region of interest from 1985–2000; sixteen of these during the 8-year span of NLOM data (1993–2000). For each cruise, the currents recorded at the shallowest depth were extracted from the archive to be representative of the surface layer currents. These depths ranged from 20–50 m. Currents sampled from NLOM represent an upper layer average with a typical thickness of ~70 m in this region. They do not contain an Ekman component and thus should be comparable to the ADCP-derived currents. Datasets were averaged into one-half- or one-quarter-degree bins for presentation, depending on the data density.

3. Results

3.1 OSCAR

OSCAR surface current plots are compiled for the region of interest. Monthly means based on eleven years of data are shown in Fig. 2. The strong westward flow of the NEC north of 10°N is consistent with the generally

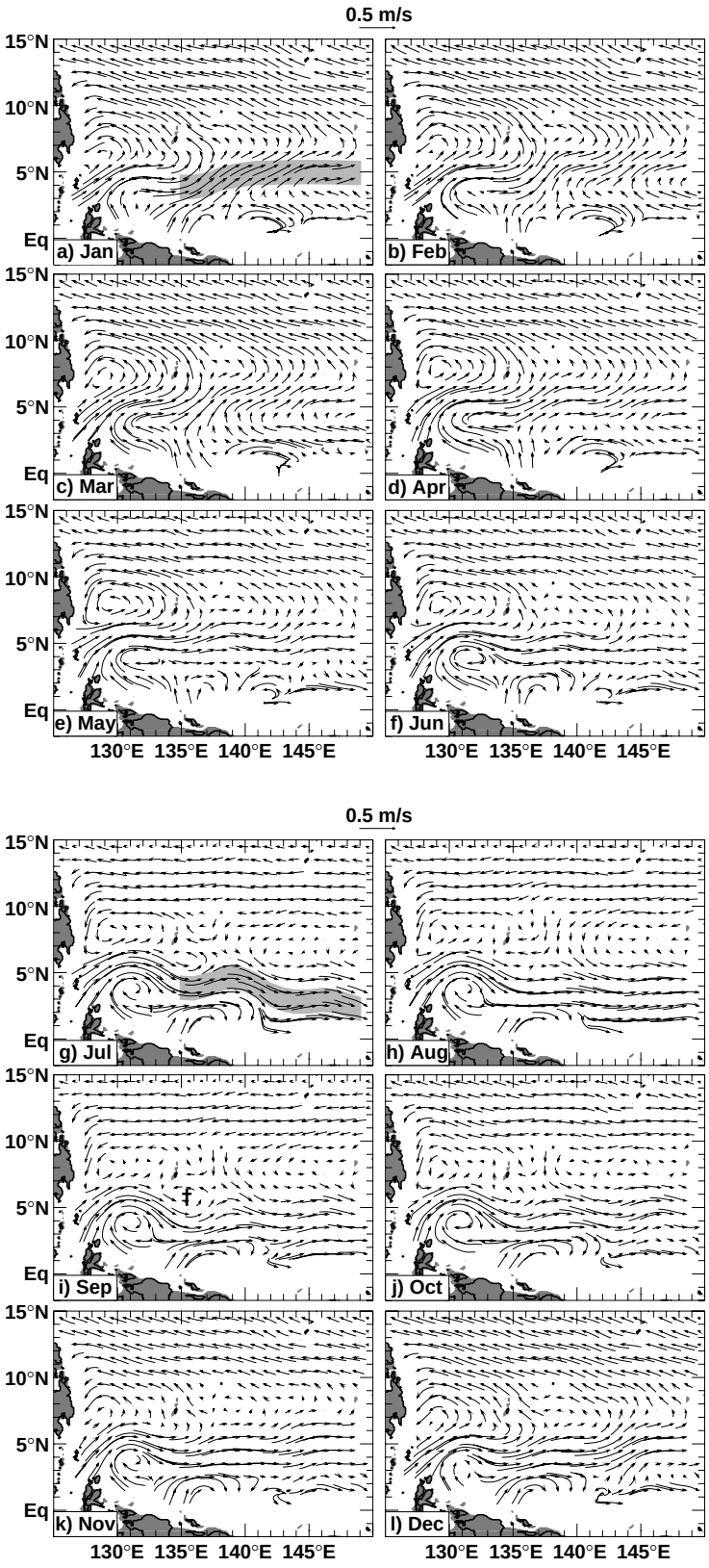

Fig. 2. Monthly mean surface currents from OSCAR plotted on the NLOM topography. Data are averaged over the period 1993–2003. (a) January, (b) February, etc. Approximate location of the MiE is identified in the September plot by the dagger (†) symbol.

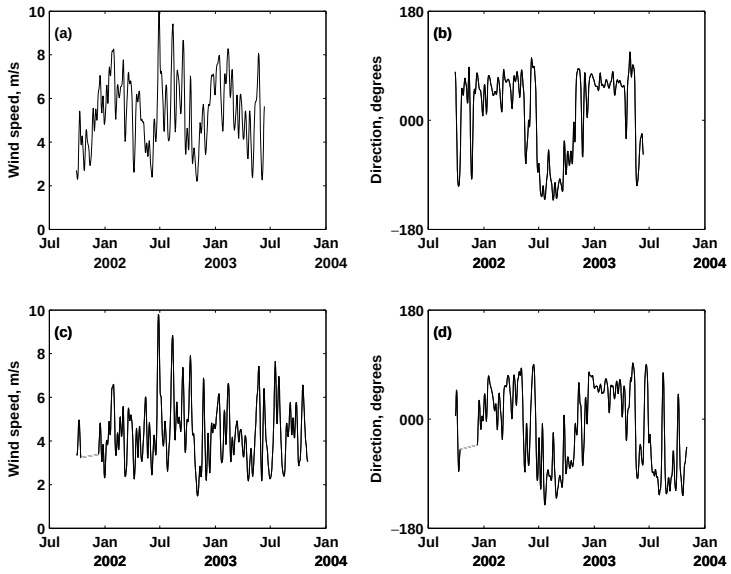

Fig. 3, TRITON buoy time series for locations: 137°E, 8°N—(a) wind speed and (b) direction. 137°E, 5°N—(c) wind speed and (d) direction.

accepted position (Gorshkov, 1976; Bramwell, 1977) with a maximum speed of 30–35 cm/s from November to March, declining to around 20–25 cm/s for July to October. During the boreal winter, there is a significant northward component to the surface current, up to 10–15 cm/s. This meridional component is reduced through spring and summer, turning southwards in late summer, and returning northwards and strengthening in winter. The timing of each of these variations is consistent with the descriptions by Yaremchuk and Qu (2004) and also that of the Asian monsoonal winds; strongest and from the northeast in winter (December–March), from the southeast during summer (June–September) (Tomczak and Godfrey, 2002).

The eastward flow of the NECC "Tail" (defined here as the section of the NECC east of 135°E) varies in position following the seasonal trend of the Asian Monsoon season (approximate positions for January and July are gray in Figs. 2(a) and (g)). From January–May, the NECC Tail is located around 5°N, consistent with literature descriptions (Tomczak and Godfrey, 2002), with maximum speeds of the order of 45 cm/s. The NECC Tail moves southward during the boreal summer to 2–5°N and is strongest (70 cm/s) during July–October when it is located at its southernmost latitudes, consistent with the findings of Toole *et al.* (1988).

During the period from December to February the cyclonic Mindanao Eddy may have developed near the Philippine coast; however, discussion of both the ME and the Mindanao Current is limited by the spatial scope of OSCAR data. From March–June the circulation of the ME is clearly seen west of Palau. The center of the eddy moves northward from 7°N in December to 8°N in July and increases its zonal dimension during this time. The ME appears to weaken from July to November, as suggested from model data by Masumoto and Yamagata (1991); as a result the zonal extent is reduced.

The spatial scope of the OSCAR system does not cover the region south of 2°N and west of 134°E, i.e., in the vicinity of Halmahera Island, and so the discussion of the Halmahera Eddy presented here is incomplete. However, the seasonal variation of HE can be deduced from the available data. During the period March–May, the eddy appears to be weakly formed. As the NECC Tail moves southwards in June, the HE becomes more clearly defined and continues to strengthen as it moves northwards, through to October. From November–February, the HE weakens and returns southwards. This annual variation is phased with the seasonality of the NECC Tail and the ME, and with that of the Asian Monsoon. The correlation in the timing of these events supports the suggestion by Toole *et al.* (1988) that the major surface currents of the western equatorial Pacific are wind-dominated. No discussion of the New Guinea Coastal Current (NGCC) can be undertaken due to the limited spatial scope of the OSCAR data near the equator.

Of note is the trace of a cyclonic eddy centered to the southeast of Palau at 136°E, 6°N during the July–September period. This previously undescribed formation, here named the Micronesian Eddy (MiE), is bounded on the south by the NECC, and the approximate location is shown by the dagger symbol in Fig. 2(i).

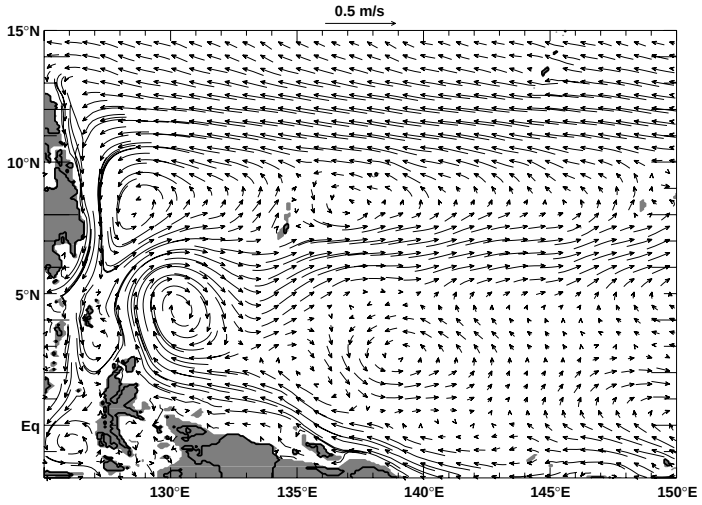

Fig. 4. NLOM annual upper layer currents averaged over the period 1993–2000. The ME is centred at 129°E, 8°N, the HE at 130°E, 4°N and the PE at 137°E, 9°N.

3.2 TRITON

Toole *et al*. (1988), Masumoto and Yamagata (1991) and Tomczak and Godfrey (2002) all assert that the major surface currents in the western equatorial Pacific are dominated by winds. Thus, wind data from the TRITON buoys are examined for periodic fluctuations to compare with the currents. Figure 3 shows wind speed and direction time-series from the buoys located at 8°N, 137°E and 5°N, 137°E. The wind direction data of the two buoys are synchronized in their seasonal variation, directed from the northeast from December to April, and from the southwest during July–October. This seasonal variation is consistent with that of the Asian monsoon (Tomczak and Godfrey, 2002). Between these dominant wind events (i.e., during May and June, and again in November), there are some short-term fluctuations in the wind direction. These times of variable wind direction generally coincide with low wind speeds. If the surface currents are wind-dominated then this observed seasonal cycle in the wind field should be reflected in the seasonality of ocean surface features.

While the OSCAR and TRITON data provide insight into the circulation in the western equatorial Pacific, more detailed information requires higher spatial (and temporal) resolutions. Numerical modelling of the ocean circulation provides a method that satisfies these requirements.

3.3 NLOM

The NLOM output is initially verified by observing the accepted western equatorial Pacific features; i.e., the NEC, ME, HE and NECC. These can be seen in the NLOM annual upper layer current climatology shown in Fig. 4. The westward-directed NEC is clearly seen north of 10°N turning southward to form the Mindanao Current around 127°E (at the Philippine coast). Part of the MC turns eastward to become the NECC, which is located at approximately 6°N. The ME, bounded by these three currents, has its dome close to the Philippine coast and extends eastwards towards Palau. The NECC is also composed of NGCC water from the southeast that has rotated around the HE, centered near 130°E, 4°N. The locations and sizes of the ME and HE, and the meandering nature of the NECC compare well with observations during WEPOCS III by Lukas *et al*. (1991) and the OSCAR data.

Figure 5 illustrates the monthly climatology from NLOM and the seasonal variations in the circulation features are observed. The description of the NEC from NLOM is generally consistent with the description from OSCAR. The NEC is located generally north of 10°N with surface current maximum speed greatest in the boreal winter (43 cm/s) and least during summer and early autumn (28 cm/s). While the maximum speeds are slightly greater than suggested by OSCAR, due perhaps to the difference in resolution, the seasonal variation is aligned. The meridional component of the NEC is greatest and northward from December to March, and turns southward during July to September.

The NECC Tail (east of 135°E) also compares favorably with the descriptions from the OSCAR data, both in magnitude and path variation; the approximate positions of the NECC Tail for January and July are gray in Figs. 5(a) and (g). The maximum surface currents for the summer and winter periods and the annual variation in the flow-rate are generally consistent with those given by OSCAR. However, the northernmost variation of the NECC Tail reaches higher latitudes (6–7°N) than those

described by OSCAR during the late winter and spring, and slightly lower latitudes (1–2°N) during late-summer/autumn. In the October–November monthly climatologies, while it appears that the NECC bifurcates at 135°E, this is not the case. Examination of each year's current maps shows that the transition between summer and winter positions can occur during October or November: the apparent bifurcation is an artifact of averaging.

In January, the ME extends southwards towards Halmahera and circulates close to the Mindanao coast, consistent with a topographic survey presented in Lukas (1988). By April, the ME has strengthened and is located adjacent to Mindanao; the meridional extent has decreased while the eddy now extends zonally to Palau. The ME begins to weaken in June and is weakest during August–September, again consistent with the annual variation suggested by the OSCAR data.

The seasonal variations in the ME seen in both NLOM and OSCAR are in contrast to the description of Wyrtki (1961), i.e., the ME is close to Mindanao in May and weakest and centered near Palau in January. This difference may be explained by the sparse data, both spatially and temporally, available to Wyrtki (1961); however, it is also possible, though seemingly unlikely, that there has been a shift in the circulation regime. The consistency between OSCAR and NLOM descriptions provide confidence in the present study.

Associated with the ME, and due to the increased spatial coverage of the model at the Philippine coast, variability of the Mindanao Current can be examined. The MC is the south-directed current produced by the bifurcation of the NEC, near the Philippine coast at 14.3 ± 0.7°N (Yaremchuk and Qu, 2004). While the NEC bifurcation may be inferred from Fig. 5, the study region does not cover these coastal waters; as such, discussion of neither the bifurcation latitude nor the meridional variation of the MC is undertaken. The zonal position of the MC is observed to vary little through the year, remaining within approximately 1° of longitude from the Mindanao coast. The speed varies from a maximum value of 1.4 m/s during the winter to 1.2 m/s during the April to November period. The MC width and surface speed are consistent with those measured by Cannon (1970) as 70–80 km and 1.1–1.3 m/s, respectively. The relatively small variation in speed through the year is consistent with the findings of Lukas (1988) that the current anomaly was in the range ±10 cm/s and with the annual variation in timing and magnitude of the MC transport described by Yaremchuk and Qu (2004). The consistency of the MC with previous studies lends further support to the reliability of the NLOM results.

The New Guinea Coastal Current between 130°E and 140°E is directed westwards for most of the annual cycle, gaining strength through May to July as a result of the increase in the South Equatorial Current (SEC) (Tomczak and Godfrey, 2002). The NGCC reaches its maximum speed in the period August to October and then diminishes through November. During December and January the NGCC reverses its direction, following the seasonal cycle of the Asian monsoon.

The Halmahera Eddy is greatly influenced by the influx of the NGCC, intensifying and increasing in size as it moves northwards during the May to September period. The HE flow dominates the waters southwest of Palau during this period. The HE begins to diminish through October and November—the same period through which the ME begins to strengthen. The HE then weakens rapidly in December with the reversal of the NGCC. This development cycle of the HE is also linked with the zonal movement of the NECC Tail, described previously.

In addition to these well-documented features, the NLOM output suggests other circulation features that influence the waters of the western equatorial Pacific. A cyclonic eddy, named the Palauan Eddy (PE), develops in April to the northeast of Palau, near 137°E, 8°N (the approximate location is shown in Fig. 5(d) by the cross symbol). The PE is bounded to the north and south by the NEC and NECC, respectively. The PE appears to be strongly correlated with the position of the NECC Tail and the abatement of the ME. The PE is strengthened during May with the northernmost attitude of the NECC Tail, and then weakens through June and July with the NECC Tail's southward migration. There is evidence of a weak regeneration of the eddy, with the return to the NECC's northern meander, from October to December. However, the PE is not visible during the January to March quarter.

An anticyclonic eddy forms in April centered near 139°E, 5°N and is designated here the Caroline Eddy (CE). The approximate location of the CE is shown in Fig. 5(d) by the plus symbol. This eddy is bounded at the north by the NECC and moves west and south in May and June as the NECC Tail migrates southwards; the CE disappears by July. Examination of each year's plots for March–June showed this feature appearing every year and propagating westward. However, as the eddy exists south of the NECC, it has no direct influence on currents near Palau and was therefore not investigated further.

A third eddy forms weakly in August and September at a meander of the NECC Tail, near 140°E, 3°N. It may be synonymous with the Micronesian Eddy (MiE) described in the OSCAR data. This cyclonic eddy strengthens in October, maintaining its position through the migration of the NECC Tail, and is present until January. Examination of each year's output for August–January showed the appearance of this feature in most, but not all, years. When formed, the eddy characteristically propagated westward. It is also important to note that the eddy

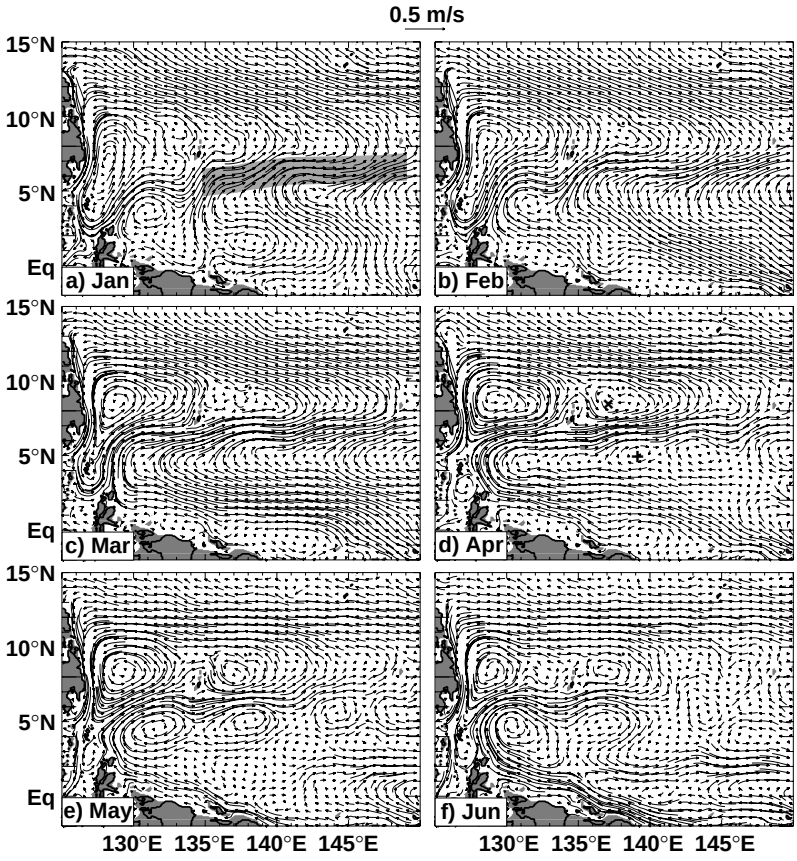

Fig. 5. Monthly mean upper layer currents from NLOM averaged over the period 1993–2000. (a) January, (b) February, etc. Approximate locations of the PE and CE are identified in the April plot by the cross (×) and plus (+) symbols, respectively.

described here may not be the same as the MiE identified in the OSCAR data. While it is located in a similar position, the spatial coverage and resolution of the OSCAR data do not permit a clear comparison. Additional studies are necessary to examine the nature and relationship of these features. As this feature is not in the vicinity of Palau, it was not investigated further.

A family of temporary eddies are also seen to form along the coast of New Guinea from July to November, between the NECC Tail and the NGCC. The formation of these eddies coincides with the greatest strength of HE, also bounded by the NECC and NGCC.

Each of the new eddies described here could be formed as a barotropic instability of the zonally-directed flows (NEC, NECC). Characteristically such instabilities propagate westwards (Rossby waves), as observed for the CE and MiE. The PE is topographically trapped by the Palau ridge (Fig. 1(b)), maintaining its position and increasing in extent and influence over the Palau waters.

While the NLOM model succeeds qualitatively in describing the surface circulation, comparison with ADCP data provides further verification.

3.4 JASADCP

Sixteen ADCP datasets with cruise tracks across the domain of interest were recorded during the 8-year span of NLOM output (1993–2000). Figure 6 shows the currents of all sixteen cruises averaged to a $0.5° \times 0.5°$ grid. The MC, ME, HE and NECC are identifiable in the sparse data and their locations compare well with the NLOM annual climatology (Fig. 4). Comparison of individual ADCP datasets with the NLOM output at the time of the cruise (i.e., not climatology) provides a more rigorous validation of the NLOM output in the western equatorial Pacific.

4. Discussion

The effects of the major currents and eddies, and their annual variations, on the circulation near Palau are summarized based on the information from OSCAR, TRITON, NLOM and the Joint Archive for Ship-based ADCP.

The OSCAR mean dynamic topography (MDT) was recently updated from a dataset that did not coincide with the 1993–2003 time period (derived from Levitus *et al.*, 1994; Levitus and Boyer, 1994) to a more rigorously de-

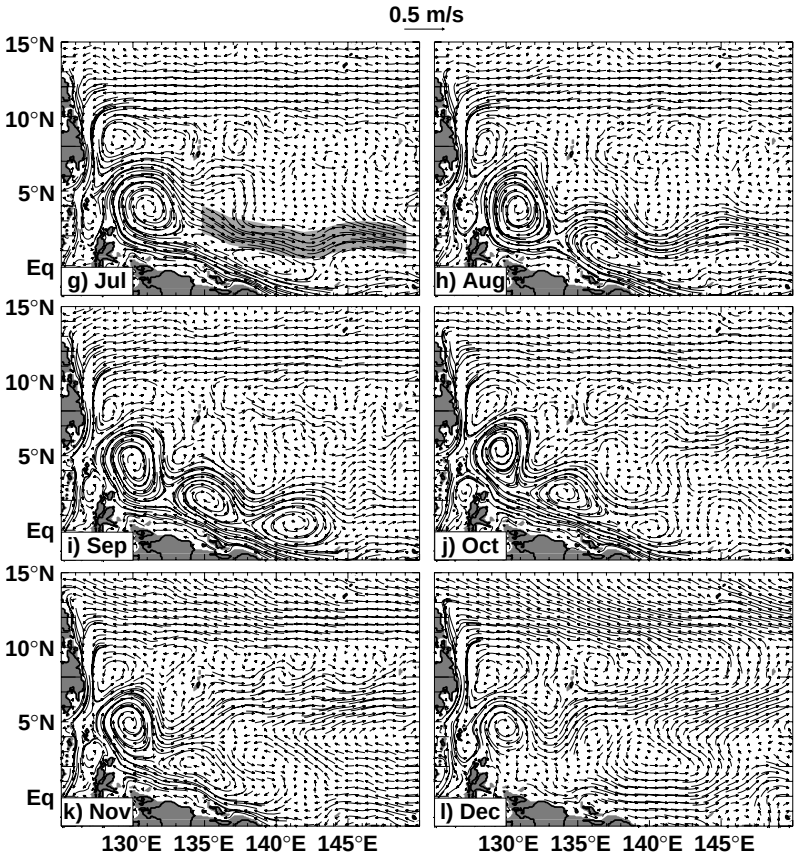

Fig. 5. (continued).

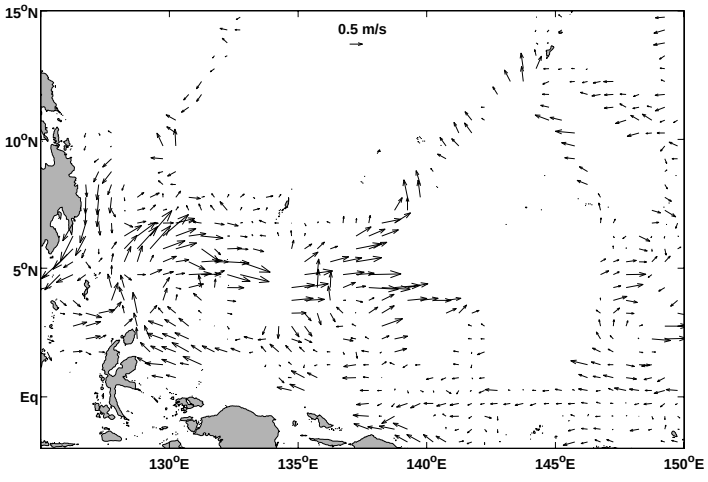

Fig. 6. Surface layer currents from ADCP measurements for the period 1993–2000. Data are averaged into 0.5° × 0.5° bins.

fined MDT that was representative of the period of OSCAR data (F. Bonjean, 2004, personal communication). This change caused a significant alteration to the vector fields and consequently to the position and extent of the major ocean features. Prior to the update, the OSCAR currents did not instill much confidence and the choice to favor the NLOM output was clear. The post-update OSCAR output showed significant visual improve-

Table 1. Vector correlation coefficients between NLOM monthly mean upper layer current climatologies and each of the pre- and post-update OSCAR monthly mean surface current climatologies.

	NLOM vs. pre-update OSCAR	NLOM vs. post-update OSCAR
Jan	0.67	0.66
Feb	0.71	0.68
Mar	0.69	0.68
Apr	0.67	0.65
May	0.63	0.58
Jun	0.62	0.57
Jul	0.62	0.63
Aug	0.62	0.65
Sep	0.52	0.53
Oct	0.48	0.43
Nov	0.55	0.52
Dec	0.62	0.64

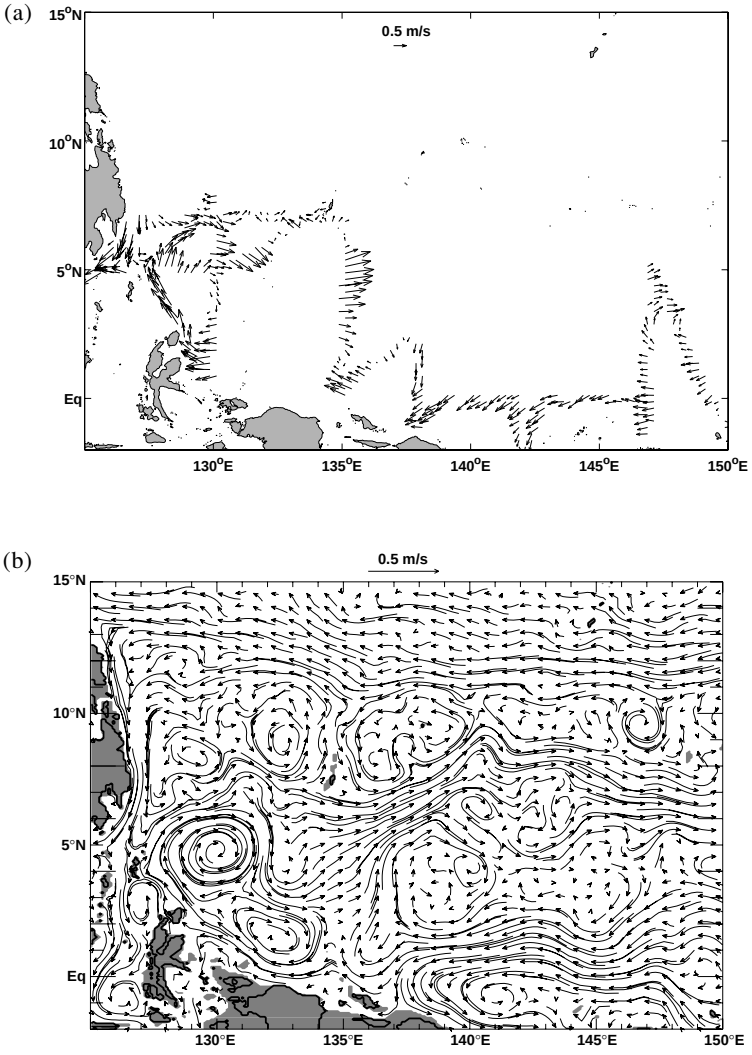

Fig. 7. (a) ADCP surface currents measured during cruise 517 (October–November 1999), averaged into 0.25° × 0.25° bins. (b) NLOM mean upper layer currents corresponding to ADCP data for cruise 517 (October–November 1999).

Table 2. Vector correlation coefficients between ADCP data and NLOM output from the same time period.

Cruise identifier	Cruise dates	Correlation with NLOM output
86	24 Jan–22 Feb 1993	0.64
138	05 Oct–09 Nov 1993	0.59
36	11 Apr–11 May 1994	0.42
535	21 Dec 1994–11 Jan 1995	0.26
483	13 Jan–23 Jan 1995	0.56
509	01–14 Jul 1995	0.74
510	23 Jan–21 Feb 1996	0.43
464	17 Jun–02 Jul 1996	0.68
511	07 Jul–04 Aug 1996	0.30
512	26 Jan–27 Feb 1997	0.28
513	29 Jul–28 Aug 1997	0.55
514	03–29 Jan 1998	0.47
515	08 Aug–08 Sep 1998	0.26
516	26 Jan–28 Feb 1999	0.69
517	21 Oct–23 Nov 1999	0.71
518	31 Aug–30 Sep 2000	0.70

ment as compared with literature studies and is the dataset presented here. In comparing the two OSCAR datasets (pre- and post-update) with the NLOM output, the new dataset appears considerably closer to that of NLOM. However, vector correlation between NLOM monthly climatologies and that of each of the OSCAR datasets resulted in very similar results. Table 1 shows the correlation coefficients; the averages of the pre- and post-update correlation coefficients are nearly identical, as are the annual variations of each. While the statistics do not reflect an improvement, the visual correlation between the post-update OSCAR and NLOM lends confidence in the more recent dataset. While it is unlikely that either of the NLOM and (post-update) OSCAR datasets are completely correct, the convergence of the information suggests they are both approaching a true representation of the western equatorial Pacific flow and that the truth is likely to lie somewhere between them.

Figures 7(a) and (b) show the ADCP data (averaged into 0.25° bins) and NLOM output, respectively, for October–November 1999. A visual comparison suggests that the model successfully replicates the position and dimension of surface features inferred from the data. The daily NLOM output was interpolated to the locations of the ADCP data points and a vector correlation between these calculated to be 0.71. Vector correlations were performed for each of the sixteen ADCP datasets and are shown in Table 2. The correlation coefficients were within the range 0.26–0.74, with a mean of 0.52. Nine values were above the mean with a further three greater than one standard deviation below the mean. Figures 8(a) and (b) shows the comparison for January–February 1997, for which a correlation coefficient of 0.28 was calculated. The NECC Tail at the longitude of Palau appears to be too far north in the NLOM output, as does the eastward flow of the NGCC. The data along the 138°E meridional transect in Fig. 8(a) may represent the eddy centered at 140°E, 2°N in the accompanying NLOM plot. For those NLOM output with poor correlations to the ADCP data, visual comparison suggests that the major features of the flow are present in the NLOM output but are displaced from the locations observed in the ADCP data. While the spatial shifting of such features is significant, the pattern of the flow given by NLOM is consistent with the ADCP data.

Of note in Fig. 8 are the strong east-directed currents at the equator. The monthly climatologies in Fig. 5 show that eastward, equatorial flow exists more weakly in the December–January climatologies and has ceased by February. While it can be postulated that this anomalous current may be related with onset of the 1997–98 ENSO event, it certainly illustrates the high variability in the western equatorial Pacific region.

While it can only be postulated that this anomalous current may be generated by west-directed winds, prior to or during the onset of the 1997–98 ENSO event, it certainly illustrates the high variability in the western equatorial Pacific region.

5. Conclusion

A seasonal variation of the currents in the waters surrounding the main islands of Palau is supported by both NLOM and OSCAR outputs. The seasonality in the TRITON wind data (i.e., December–April and July–October) is mirrored by the circulation around Palau.

During the period December to April, the currents at Palau are influenced by the NECC and the ME. The posi-

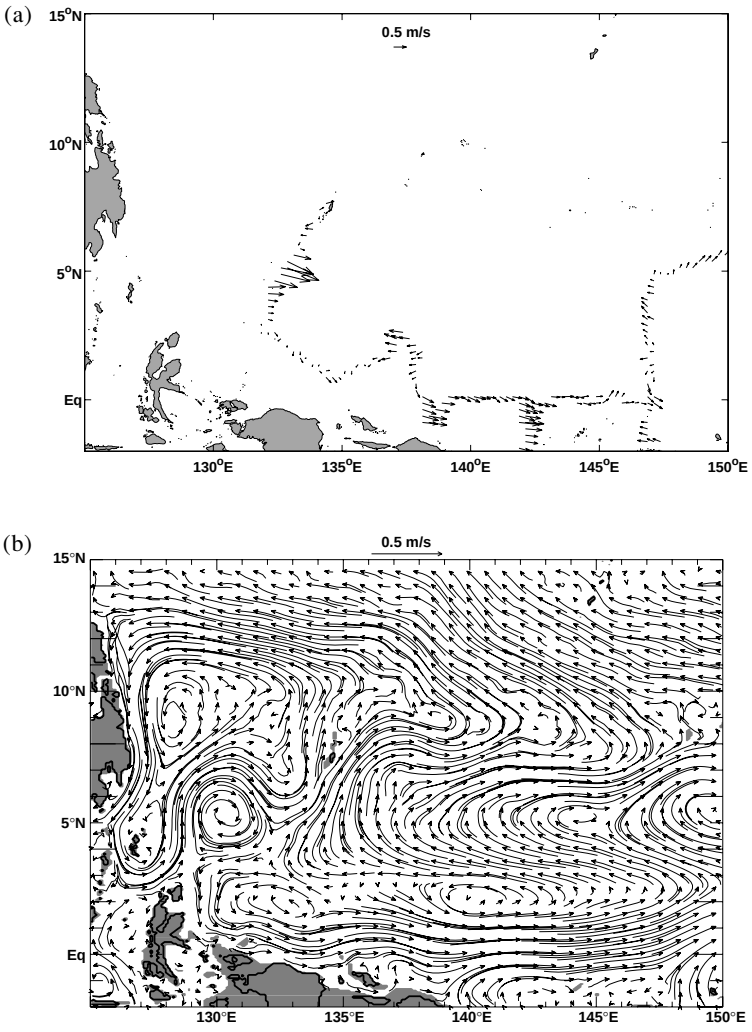

Fig. 8. As Fig. 7, except for cruise 512 (January–February 1997).

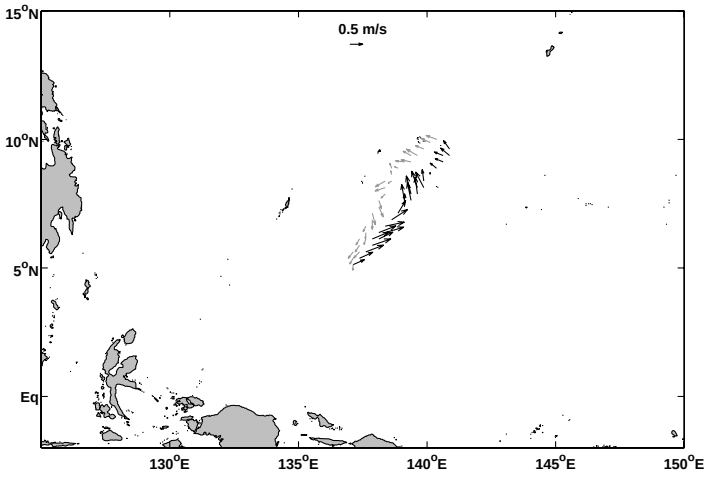

Fig. 9. ADCP surface currents measured during cruise 036 (April–May 1994, black) and cruise 037 (April–May 1992, gray) in the vicinity of the Palau Eddy (cf. Fig. 4). Data from each cruise is averaged into 0.25° × 0.25° bins.

tions of the ME and NECC Tail are generally farther north in the NLOM output than that given by OSCAR. The Palauan currents described by NLOM are dominated by the NECC and are directed more towards the northeast; OSCAR currents are dominated by the ME and thus deflect more towards the northwest. The direction of the TRITON wind data for this period is from the northeast. Accounting for the Ekman-shift between wind and current directions, this suggests that the surface water transport will be directed towards the north and northwest. Combining these pieces of information suggests that the current is generally directed to the north in this period. The speed of the current for this period, according to both NLOM and OSCAR, is around 20 cm/s.

Both data sets indicate the effect of the ME upon the currents to the west of Palau through the December to April period. The currents curve with the shape of the ME, from northeast to northwest, with increasing latitude. As the ME migrates northwards through this period, the directions of the currents turn clockwise. As the ME decreases in its meridional extent (from April onwards), its effect on the Palauan currents is reduced.

The NLOM output suggests the formation of the PE in April; however, this eddy is not observed in the OSCAR output. This may be due to the lower spatial resolution of OSCAR. The existence of the PE would affect the currents along the east coast of Palau through significant portions of the year. ADCP data for April–May 1992 and April–May 1994, shown in Fig. 9, supports the existence of a cyclonic circulation (the PE) at a similar location as indicated by the NLOM climatology (Fig. 4).

During April and May, the PE directs currents along the east coast of Palau to the south with speeds up to 25 cm/s. With the southward migration of the NECC Tail in June, the currents east of Palau are less directionally defined and reduced in magnitude to less than 15 cm/s. West of Palau the ME continues to weaken, resulting in north-directed currents of approximately 10–15 cm/s.

During the period July to September, the major surface features do not affect the waters around Palau and the circulation becomes somewhat disordered. The flow shows a tendency to the north along the west coast and to the south along the east coast. The magnitude of the currents is around 5 cm/s. With the regeneration of the PE in October, the south-directed current along the eastcoast increases to 15 cm/s. In November the currents begin the transition to their north-directed winter pattern with the return of the NECC Tail to its northern path.

The seasonal variation of the surface circulation in the western equatorial Pacific is linked to the Asian monsoon cycle and is dependent upon the major surface features of the region. Observational data were used to validate numerical model output in the region and, together, these have confirmed the locations and annual variations of the established surface features. Previously undescribed, transient eddies (named here the Palau Eddy, Caroline Eddy and Micronesian Eddy) have been identified and their seasonality discussed. The flow in the immediate vicinity of Palau is affected by many of these features.

This description of the currents is the first known study of the variability of circulation around Palau and thus forms a basis for oceanographic studies of Palauan waters. The currents described provide insight into studies of biological connectivity and may be applied as far-field boundary conditions for high resolution numerical models of Palau. The identification of transient eddies, in both location and seasonal duration, from the model output provides a sensible guide for future studies to obtain *in situ* data.

Acknowledgements

OSCAR data were provided by NOAA/NESDIS under the National Oceanographic Partnership Program. Thanks to the TRITON Project Office (Dr. Yoshifumi Kuroda, Director) for the buoy data and to the JASADCP for the ADCP data archive. This work was performed as part of the 6.1 Dynamics of Low Latitude Western Boundary Currents project under program element 601153N sponsored by the Office of Naval Research. The numerical simulation was performed using a grant of computer time from the Department of Defense High Performance Computing Modernization Office on the Cray T3E computer at the Naval Oceanographic Office, Stennis Space Center, Mississippi. Thanks to Tamara Townsend (NRL) who performed the NLOM simulation used here. This work was funded, in part, by The Nature Conservancy, including a contribution from the Michael and Andrea Banks Nature Fund. Thanks to Al Strong and Eric Bayler whose comments improved the manuscript.

References

Arief, D. and S. P. Murray (1996): Low-frequency fluctuations in the Indonesian throughflow through Lombok Strait. *J. Geophys. Res.*, **101**, 12455–12464.

Bonjean, F. and G. S. E. Lagerloef (2002): Diagnostic model and analysis of the surface currents in the tropical Pacific Ocean. *J. Phys. Oceanogr.*, **32**, 2938–2954.

Bramwell, M. (ed.) (1977): *The Atlas of the Oceans*. Mitchell Beazley Publishers Ltd, London, p. 162–163.

Cannon, G. A. (1970): Characteristics of waters east of Mindanao, Philippine Islands, August 1965. p. 205–211. In *The Kuroshio, A Symposium on the Japan Current*, ed. by J. C. Marr, East-West Center Press, Honolulu.

Gorshkov, S. G. (ed.) (1976): *World Ocean Atlas, Volume 1—Pacific Ocean*. Pergamon Press, Oxford, p. 204–207.

Kashino, Y., E. Firing, P. Hacker, A. Sulaiman and Lukiyanto (2001): Currents in the Celebes and Maluku Seas, February 1999. *Geophys. Res. Lett.*, **28**, 1263–1266.

Levitus, S. and T. P. Boyer (1994): *World Ocean Atlas 1994. Vol. 4, Temperature*. NOAA Atlas NESDIS 4, NOAA, Washington, D.C., 117 pp.

Levitus, S., R. Burgett and T. P. Boyer (1994): *World Ocean Atlas 1994. Vol. 3, Salinity*. NOAA Atlas NESDIS 3, NOAA, Washington, D.C., 99 pp.

Lukas, R. (1988): Interannual fluctuations of the Mindanao Current inferred from sea level. *J. Geophys. Res.*, **93**, 6744–6748.

Lukas, R., E. Firing, P. Hacker, P. L. Richardson, C. A. Collins, R. Fine and R. Gammon (1991): Observations of the Mindanao Current during the Western Equatorial Pacific Ocean Circulation Study. *J. Geophys. Res.*, **96**, 7089–7104.

Masumoto, Y. and T. Yamagata (1991): Response of the Western Tropical Pacific to the Asia Winter Monsoon: The generation of the Mindanao Dome. *J. Phys. Oceanogr.*, **21**, 1386–1398.

Metzger, E. J. (2003): Upper ocean sensitivity to wind forcing in the South China Sea. *J. Oceanogr.*, **59**, 783–798.

Metzger, E. J., H. E. Hurlburt, J. C. Kindle, Z. Sirkes and J. M. Pringle (1992): Hindcasting of wind-driven anomalies using a reduced gravity global ocean model. *Mar. Technol. Soc. J.*, **26**(2), 23–32.

Qiu, B. and R. Lukas (1996): Seasonal and interannual variability of the North Equatorial Current, the Mindanao Current, and the Kuroshio along the Pacific western boundary. *J. Geophys. Res.*, **101**, 12315–12330.

Qu, T. and R. Lukas (2003): The bifurcation of the North Equatorial Current in the Pacific. *J. Phys. Oceanogr.*, **33**, 5–18.

Qu, T., H. Mitsudera and T. Yamagata (1998): On the western boundary currents in the Philippines Sea. *J. Geophys. Res.*, **103**, 7537–7548.

Smedstad, O. M., H. E. Hurlburt, E. J. Metzger, R. C. Rhodes, J. F. Shriver, A. J. Wallcraft and A. B. Kara (2003): An operational eddy resolving 1/16° global ocean nowcast/forecast system. *J. Mar. Sys.*, **40–41**, 341–361.

Smith, W. H. F. and D. T. Sandwell (1997): Global sea floor topography from satellite altimetry and ship depth soundings. *Science*, **277**, 1956–1962.

Tomczak, M. and J. S. Godfrey (2002): *Regional Oceanography: An Introduction*. Online publication (http://www.es.flinders.edu.au/~mattom/regoc/pdfversion.html).

Toole, J. M., E. Zou and R. C. Millard (1988): On the circulation of the upper waters in the western equatorial Pacific Ocean. *Deep-Sea Res.*, **35**, 1451–1482.

Wyrtki, K. (1961): *Naga Report, Volume 2—Physical Oceanography of the Southeast Asian Waters*. Scripps Institution of Oceanography, La Jolla, U.S.A., 195 pp.

Yaremchuk, M. and T. Qu (2004): Seasonal variability of the large-scale currents near the coast of the Philippines. *J. Phys. Oceanogr.*, **34**, 844–855.